

## Steady-state substrate specificity and O<sub>2</sub>-coupling efficiency of mouse cysteine dioxygenase<sup>☆</sup>



Wei Li, Brad S. Pierce<sup>\*</sup>

Department of Chemistry and Biochemistry, College of Sciences, The University of Texas at Arlington, Arlington, TX 76019, United States

### ARTICLE INFO

#### Article history:

Received 3 September 2014  
and in revised form 7 November 2014  
Available online 20 November 2014

#### Keywords:

Non-heme iron  
Cysteine  
Dioxygenase  
Specificity  
Coupling  
Thiols

### ABSTRACT

Cysteine dioxygenase (CDO) is a non-heme mononuclear iron enzyme that catalyzes the oxygen-dependent oxidation of L-cysteine (Cys) to produce L-cysteine sulfinic acid (CSA). Sequence alignment of mammalian CDO with recently discovered thiol dioxygenase enzymes suggests that the mononuclear iron site within all enzymes in this class share a common 3-His first coordination sphere. This implies a similar mechanistic paradigm among thiol dioxygenase enzymes. Although steady-state studies were first reported for mammalian CDO over 45 years ago, detailed analysis of the specificity for alternative thiol-bearing substrates and their oxidative coupling efficiencies have not been reported for this enzyme. Assuming a similar mechanistic theme among this class of enzymes, characterization of the CDO substrate specificity may provide valuable insight into substrate-active site intermolecular during thiol oxidation. In this work, the substrate-specificity for wild-type *Mus musculus* CDO was investigated using NMR spectroscopy and LC-MS for a variety of thiol-bearing substrates. Tandem mass spectrometry was used to confirm dioxygenase activity for each non-native substrate investigated. Steady-state Michaelis–Menten parameters for sulfinic acid product formation and O<sub>2</sub>-consumption were compared to establish the coupling efficiency for each reaction. In light of these results, the minimal substrate requirements for CDO catalysis and O<sub>2</sub>-activation are discussed.

© 2014 Elsevier Inc. All rights reserved.

### Introduction

Cysteine dioxygenase (CDO)<sup>1</sup> is a mononuclear non-heme iron enzyme that catalyzes the first concerted step in the O<sub>2</sub>-dependent oxidation of L-cysteine (Cys) to produce cysteine sulfinic acid (CSA) (Scheme 1). Enzymes involved in sulfur-oxidation and transfer are increasingly being recognized as potential drug targets for development of antimicrobials, therapies for cancer, and inflammatory

disease [1–4]. Recently, the interplay between dysfunction in sulfur metabolism and human neurodegenerative disease states (Alzheimers, autism, and Parkinsons) has been of considerable medical interest [5–7].

Multiple high resolution crystal structures of the resting and substrate-bound enzyme have been solved which highlight the atypical mononuclear iron coordination for the mammalian CDO active site [6,8–10]. Among the non-heme mononuclear iron oxidase/oxygenase class of enzymes, the typical Fe-coordination sphere is comprised of two protein-derived neutral His residues and one monoanionic carboxylate ligand provided by either an Asp or Glu residue. Unlike most enzymes within this family, one face of the CDO mononuclear iron active site (Fig. 1) is coordinated by 3 protein derived histidine residues resulting in a 3-His facial triad. Another unusual feature observed within the mature eukaryotic CDO active site is a post-translational modification in which spatially adjacent Cys93 and Tyr157 residues are covalently cross-linked to produce a C93-Y157 pair. Among CDO enzymes identified, Y157 is conserved across phylogenetic domains whereas the C93-Y157 pair is unique to eukaryotes. Several reports have demonstrated that formation of this cross-link increases the catalytic activity and coupling efficiency of CDO [11–13]. Regardless, C93A CDO variants, which lack the ability to produce the

<sup>☆</sup> This work was supported by the National Science Foundation (CHE) 1213655 (B.S.P.).

<sup>\*</sup> Corresponding author at: Department of Chemistry and Biochemistry, 700 Planetarium Place, Room 130, The University of Texas at Arlington, Arlington, TX 76019, United States. Fax: +1 (817) 272 3808.

E-mail address: [bspierce@uta.edu](mailto:bspierce@uta.edu) (B.S. Pierce).

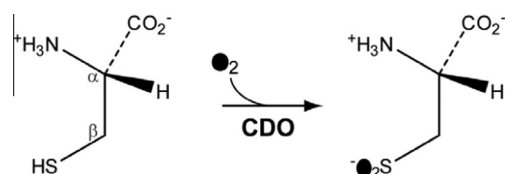
<sup>1</sup> Abbreviations used: TDO, thiol dioxygenase; CDO, cysteine dioxygenase; ADO, cysteamine dioxygenase; MSDO, mercaptosuccinate dioxygenase; MPDO, 3-mercaptopropanoate dioxygenase; Cys, cysteine; Hcy, homocysteine; CA, 2-aminoethanethiol (cysteamine); MS, mercaptosuccinate; PA, L-penicillamine; CME, L-cysteine methyl ester; DME, 2-(dimethylamino)ethanethiol; SC, S-methyl-L-cysteine; 3MP, 3-mercaptopropanoate; 1MP; 1-mercaptopropane; HT, hypotaurine; TMSp, trimethylsilyl propanoic acid; TCEP, tris(2-carboxyethyl)phosphine hydrochloride; HPLC, high performance liquid chromatography; NMR, nuclear magnetic resonance; LC-MS, liquid chromatography-mass spectrometry; MRM, multiple reaction monitoring; SIM, single ion mode.

C93-Y157 pair, retain their catalytic activity. Therefore, this post-translational modification does not appear to be required for catalysis. The exact mechanism of C93-Y157 formation remains unresolved.

As shown in Fig. 1, the L-Cys substrate coordinates to the Fe-site in a bidentate manner via neutral amine and thiolate functional groups [10]. Like other members of the non-heme mononuclear iron enzyme family, CDO exhibits an obligate-ordered binding of the L-Cys substrate prior to molecular oxygen [14,15].

Cysteine dioxygenase and cysteamine (2-aminoethanethiol) dioxygenase (ADO) are the only known mammalian thiol dioxygenase (TDO) enzymes. Until recently, the catabolic dissimilation of L-cysteine was believed to be unique within the domain of eukaryotes [16,17]. However, a number of bacterial TDO enzymes have now been identified, suggesting that the ability to oxidize excess thiols is advantageous for survival. For example, two Fe/O<sub>2</sub>-dependent TDO enzymes isolated from *Variovorax paradoxus* have recently been identified [mercaptosuccinate dioxygenase, (MSDO) and 3-mercaptopropionate dioxygenase (MPDO)] [18,19]. Sequence comparison suggests these enzymes also contain a 3-His active site motif. The conserved metal binding site among TDO enzymes suggest that the first-coordination sphere is necessary for thiol oxidation whereas the outer-sphere residues most likely facilitate binding of their specific substrates. This implies that TDO enzymes have the potential to catalyze the O<sub>2</sub>-dependent oxidation of a variety of thiol-substrates to produce the corresponding sulfinic acid providing they are capable of binding to the mononuclear active site.

All TDO enzymes identified belong to the cupin superfamily which is defined on the basis of a characteristic β-barrel tertiary structure. Despite significant deviations in thiol-substrates and amino acid sequence homology, several conserved features can be identified among TDO enzymes. A sequence alignment for selected TDO enzymes is provided in Supplemental information, Fig. S1. From this analysis, the 3-His active site motif appears to be a common feature among TDO enzymes. Beyond the active site 3-His residues, several conserved residues are observed in CDO enzymes across phylogenetic domains (Y58, R60, H155, and Y157). For example, Y157 and H155 residues are present in both eukaryotic and prokaryotic enzyme forms. Moreover, both Y157F and H155A CDO variants exhibit abolished (or minimal) enzymatic activity [20,21]. Recent spectroscopic experiments on the catalytically inactive ferric enzyme suggest that these residues are involved in key outer-sphere interactions with the substrate-bound active site to facilitate catalysis. By contrast, the C93 involved in C93-Y157 cross-link formation is only observed in mammalian CDO enzymes. In bacterial enzymes this residue is replaced by a glycine suggesting that this cross-link is not catalytically essential. In support of this hypothesis, C93A and C93S variants of mammalian CDO retain catalytic activity, albeit with decreased *k<sub>cat</sub>* [13,20]. X-ray crystallography and computational models suggest that R60 is involved in charge stabilizing of the L-Cys carboxylate group. This Arg residue is absent in mammalian and bacterial ADO enzymes which catalyze the O<sub>2</sub>-dependent oxidation of 2-aminoethanethiol (cysteamine). It has also been noted that Ser153, His155 and Tyr157 may form a “catalytic triad” similar to those observed among hydrolase or transferase enzymes [22].



Scheme 1. CDO catalyzed oxidation of L-cysteine to produce cysteine sulfinic acid.

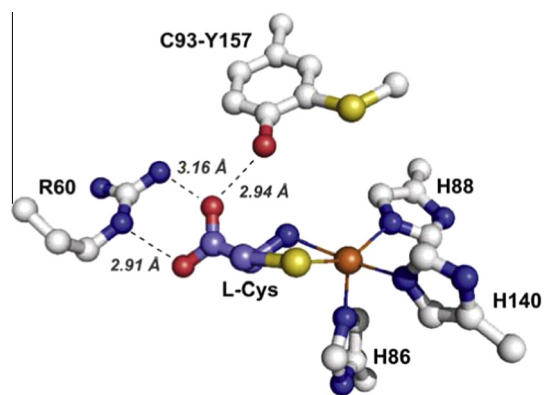


Fig. 1. 1.60 Å resolution X-ray crystal structure for the substrate-bound CDO active site at pH 8.0 (pdb code 4IEV) [10].

This seems unlikely as S153 is not universally conserved across phylogenetic domains similar to H155 and Y157. No experiments to date provide any insight into the catalytic role of these residues.

Previous studies suggest that mammalian CDO exhibits high substrate and stereoselectivity [23–26]. For example, it has been reported that L-homocysteine is an inhibitor of CDO but its potential as a substrate has not been carefully evaluated [27]. In fact detailed characterization of any non-natural substrates is severely underreported. In this work, a variety of commercially available thiol-substrates were utilized to evaluate the substrate-specificity of wild-type CDO cloned from *Mus musculus*. Substrates were selected to evaluate specific active site interactions and cross-reactivity among other physiological TDO substrates [ADO (cysteamine), MPDO (3-mercaptopropionate), and MSDO (mercaptosuccinate)]. The steady-state kinetic parameters and coupling efficiencies for O<sub>2</sub>-consumption and sulfinic acid formation are reported. In all substrates evaluated, NMR spectroscopy, differential <sup>16</sup>O/<sup>18</sup>O-incorporation, and tandem LC–MS/MS were employed to confirm formation of the appropriate sulfinic acid product.

## Materials and methods

### Enzyme purification

Recombinant mouse CDO was expressed in *Escherichia coli* BL21(DE3) pLysS competent cells (Novagen) and purified using a 10 L bioreactor (New Brunswick Scientific Bioflo100) as previously described [14]. The as-isolated CDO enzyme typically contains ~50% (±10%) of the C93-Y157 cross-link as observed by SDS PAGE. Therefore, prior to use, isolated CDO is converted to the fully modified enzyme as described elsewhere [13]. All preparations were assayed for ferrous and ferric iron content spectrophotometrically as previously described [15,28]. Typical ferrous iron incorporation within purified CDO is ~70% (±10%). For clarity, the concentrations reported in enzymatic assays reflect the concentration of ferrous iron within samples of CDO (Fe<sup>II</sup>-CDO).

### NMR kinetic study

NMR kinetic studies were performed on a 300 JEOL nuclear magnetic resonance spectrometer (Pleasanton, CA). All measurements were made in Wilmad NMR tubes (standard wall, 5 mm O.D., precision, 507-PP-7). For each reaction, fully modified CDO (typically 2–25 μM) was added to a buffered substrate solution in D<sub>2</sub>O (sodium phosphate buffer, 50 mM NaCl, pD 7.5) to initiate the reaction at ambient temperature (20 ± 2 °C). Reaction points were terminated by heat shock at 95 °C for 2 min followed by spin-filtration to remove denatured protein. Final concentration

of 1 mM trimethylsilyl propanoic acid (TMSP) was added as the internal standard. NMR spectra were integrated using JOEL USA Delta NMR data processing software (version 5.0.4). The corrected value of pD was obtained by adding 0.4 pD units to the value reported by the pH electrode (Mettler Toledo InLab Expert Pro) [29].

#### Circular dichroism (CD)

CD analysis of CDO in H<sub>2</sub>O and D<sub>2</sub>O buffer was performed on JASCO 715 UV–visible circular dichroism spectrometer with xenon arc light source. Protein samples analyzed by CD were prepared in 10 mM phosphate buffer, 50 mM NaCl, pL 7.5 filtered through a 0.22 μm polypropylene membrane filter (VWR international). Equine heart myoglobin (100684-32-0), chicken egg white lysozyme (12650-88-3), and poly-L-lysine (25988-63-0) purchased from Sigma–Aldrich were used as standards for secondary structure determination as described elsewhere [30]. CD results were also interpreted using the freely available online software K2D3 (<http://k2d3.ogic.ca/>). Far-UV (185–260 nm) CD spectra were recorded in a quartz cuvette of 0.1 cm path length and ~0.45 mL volume at a scan speed of 40 nm/min at 20 ± 2 °C.

#### Oxygen electrode

The rate of dissolved oxygen consumption utilized in CDO reactions was determined using a standard Clark type electrode (Hansatech Instruments, Norfolk, England). Reaction temperatures were maintained at 20 ± 2 °C using a circulating water bath (ThermoFlex 900, Thermo Scientific). Calibration of the O<sub>2</sub>-electrode was performed as previously described [13]. For each potential CDO substrate utilized, 1.0 mL of a stock substrate solution was prepared in a buffered solution (25 mM HEPES pH 7.5 or equivalent phosphate buffer), and incubated at 20 °C for 3–5 min to equilibrate the reaction solution to the cell temperature and establish a baseline for O<sub>2</sub>-electrode. Reactions were initiated by addition of CDO to obtain a final enzyme concentration within the cell of 1 μM.

#### <sup>18</sup>O<sub>2</sub> enzymatic reactions

Enzyme and substrate solutions were rigorously degassed on a Schlenk line prior to transferring into the anaerobic chamber. Analytical grade argon was passed through a copper catalyst (Kontes, Vineland, N.J.) to remove atmospheric <sup>16</sup>O<sub>2</sub> impurities and then sparged through distilled water to hydrate gas. All anaerobic samples were prepared within sealed vials in a glove box (Coy Laboratory Products Inc., Grass City, MI) with the O<sub>2</sub> concentration maintained below 1 ppm. <sup>18</sup>O<sub>2</sub> reactions were prepared within the anaerobic chamber by adding excess substrate (25 mM) to a 15 mL tube (VWR Catalog Number 89049-170) containing 5.0 μM CDO. Each vial was sealed using a rubber septum (ChemGlass P/N CG-3022-93) within the glove box and secured by standard electrical tape. <sup>18</sup>O<sub>2</sub>-saturated buffer (99%) was prepared by sparging anaerobic buffer with <sup>18</sup>O<sub>2</sub> gas (Icon 99% <sup>18</sup>O<sub>2</sub>, P/N 11135). For all substrates, 500 μL of the <sup>18</sup>O<sub>2</sub>-saturated buffer was spiked into the septum sealed reaction vial by gas-tight Hamilton syringe resulting in an approximate final O<sub>2</sub> concentration of ~226 μM [31]. Reaction mixtures were mixed by gentle inversion and allowed to react for >1 h prior to heat denaturation, spin-filtration, and work up for LC–MS analysis.

#### HPLC analysis

CDO catalyzed oxidation of L/D-cysteine and 2-aminoethanethiol (cysteamine) was performed by isocratic reverse phase HPLC

as previously described [13,14]. Instrumentation: Shimadzu LCMS-2020; Column, Phenomenex Kinetex C18, 100 Å column 100 × 4.6 mm, 2.6 μm; Mobile phase, 20 mM sodium acetate, 0.6% methanol, 1% heptafluorobutyric acid, pH 2.0; Injection volume, 50 μL; Flow rate, 1.0 mL/min. Product CSA and hypotaurine peaks were detected spectrophotometrically at 218 nm. Each reaction was initiated by addition of enzyme (1 μM) to a buffered solution (25 mM phosphate, 50 mM NaCl, pD 7.5) containing substrate at ambient temperature (20 ± 2 °C). At selected times, aliquots were collected and quenched by addition of 10 μL of 40 mM hydrochloric acid. Following addition of HCl, samples were heated to 95 °C for 3 min to ensure full enzyme denaturation and then spin-filtered by 0.22 μm cellulose acetate membrane (Corning, Spin-X) prior to analysis on HPLC. The concentration of CSA and hypotaurine produced in reactions were determined by comparison to standard calibration curves (0.1–20 mM). Steady-state kinetic parameters for CDO were determined by fitting data to the Michaelis–Menten equation using the program SigmaPlot ver. 11.0 (Systat Software Inc., Chicago, IL).

#### LC–MS and LC–MS/MS analysis

Detection and verification of enzymatic products were performed on a triple quadrupole LC–MS/MS (Shimadzu Scientific Instruments, LC–MS 8040) in positive ion mode. Instrumentation: Column, Phenomenex Luna 3 μm HILIC 200Å, 100 × 2.00 mm, (P/N OOD-4449-B0); Mobile phase, 70% ACN, 30% H<sub>2</sub>O, 30 mM NH<sub>4</sub>AC, 0.1% trifluoroacetic acid; Injection volume, 2 μL; flow rate, 0.25 mL/min. Confirmation of CDO product was verified multiple reaction monitoring (MRM) using a triple quadrupole LC–MS/MS [Shimadzu Scientific Instruments, LCMS 8040] [32,33]. The molecular ions (M<sup>+</sup>) of the CDO products (CSA, 154 m/z and hypotaurine, 110 m/z) were selected for secondary fragmentation. MRM optimization was then employed to maximize transition intensity and sensitivity for each fragment. The optimized MRM method was used to verify both substrate and product by direct injection of enzymatic assays. These results were compared to direct injection of standards.

Additional verification of dioxygenase activity was confirmed by select ion mode (SIM) in LC–MS. In these experiments, the mass of the molecular ion (M<sup>+</sup>) was compared following the exchange of <sup>16</sup>O<sub>2</sub> molecular oxygen for <sup>18</sup>O<sub>2</sub>. Incorporation of both oxygen atoms into the substrate should result in an increase in the molecular ion of 4 m/z.

## Results

#### Validation of CDO steady-state kinetics utilizing native (L-Cys) substrate by NMR, O<sub>2</sub>-electrode, and mass spectrometry

The rate of CDO catalyzed L-cysteine oxidation to produce CSA has been well characterized by utilizing both HPLC, O<sub>2</sub>-electrode, and LC–MS [8,13,34]. While significantly less sensitive than these methods, NMR does offer a greater flexibility in monitoring a potentially broad range of sulfenic acids produced by CDO. Moreover, re-optimization of mobile phase or assay conditions for each individual substrate is time consuming and impractical. Since NMR has not previously been utilized to study CDO activity, it is important to first validate this method using the native CDO substrate (L-Cys) prior to proceeding to non-native substrates.

As an initial point of comparison, the NMR spectra for L-cysteine and CSA standards within a sodium phosphate buffer in D<sub>2</sub>O (pD 7.5) are shown in Supplemental Information, Fig. S2 (panel A). Within this spectral window (2.50–4.40 ppm), only the non-exchangeable protons on the α- and β-carbons (Scheme 1) are observed. Both have clearly resolved resonances which can be utilized to monitor either

the formation of CSA or loss of L-Cys over the course of a typical reaction. The NMR spectra of L-Cys exhibits three sets of resonances observed as a doublet of doublets (*dd*) centered at 3.02, 3.10, and 3.97 ppm. By comparison, the same  $\alpha/\beta$ -protons observed for CSA are observed at 2.70, 2.84, and 4.16 ppm. Relative to the L-Cys starting material, the diastereotopic protons on the  $\beta$ -carbon exhibit the greatest overall change in chemical shift due to the close proximity of the adjacent sulfinic acid group. For simplicity, the  $\alpha$ -proton for L-Cys and CSA (3.97 and 4.16 ppm, respectively) were utilized to monitor the rate of CDO catalyzed CSA formation.

To demonstrate the utility of NMR spectroscopy for monitoring the steady state kinetics for CDO catalyzed reactions, both the decay of L-Cys and formation of CSA were monitored with time. Each reaction was initiated by addition of CDO (0.5  $\mu$ M) to a buffered D<sub>2</sub>O solution (25 mM phosphate, 50 mM NaCl, pD 7.5, 20 °C) containing 4.5 mM L-Cys. At selected time points, samples were quenched, spin-filtered, and analyzed by NMR spectroscopy. Trimethylsilyl propanoic acid (TMSP) was added as an internal standard to each sample for normalization of signal intensity as described in Material and Methods. Representative NMR spectra for the CDO catalyzed formation of CSA are shown in Supporting Information, Fig. S2 (panel B). Quantitation of each species was performed by comparison of the integrated peak area to freshly prepared standards of known concentration. Fig. 2A shows the time-dependent integrated results for L-Cys and CSA ( $\alpha$ -protons). Data were fit to either a single exponential decay (L-Cys) or a single exponential rise to maximum (CSA) using the same observed rate constant ( $k_{obs} \sim 0.12 \pm 0.03 \text{ h}^{-1}$ ). The amplitude (*A*) of the exponential phase was  $4.0 \pm 0.15 \text{ mM}$ , representing  $\sim 88\%$  of theoretical value (4.5 mM). The initial velocity ( $v_0$ ) is obtained from the product of the reaction amplitude and rate constant ( $v_0 = k_{obs} \cdot A$ ). By normalizing this value by the concentration of enzyme (0.5  $\mu$ M), the initial velocity for CSA formation at 4.5 mM L-Cys is obtained ( $v_0/[E] = 0.27 \pm 0.07 \text{ s}^{-1}$ ). These results indicate that over the course of this reaction, nearly stoichiometric formation of CSA is observed and its rate of formation is kinetically matched to the loss of L-Cys.

Using this method, steady state kinetics for CDO catalyzed CSA formation were performed as described above while varying the concentration of L-Cys from 1 to 20 mM. Rather than monitor reactions over an extended time as described above, the initial rate ( $v_0$ ) of each reaction was collected within the linear regime of product formation ( $\sim 45$ -min). To compensate for shorter reaction times, the enzyme concentration was increased to 4  $\mu$ M. As before, all initial rates are normalized for Fe-containing enzyme concentration

( $v_0/[E]$ ), such that the values for  $k_{cat}$  and  $K_M$  are easily obtained from fitting the results to the Michaelis–Menten equation. The steady-state kinetics for wild-type CDO with L-Cys obtained by NMR spectroscopy is shown in Fig. 2B. The solid line represents a best-fit to the initial rate of CSA formation ( $\square$ ) as a function of substrate concentration. From this analysis, the  $k_{cat}$  and  $K_M$  values for CSA formation were determined to be  $0.74 \pm 0.06 \text{ s}^{-1}$  and  $7.3 \pm 1.5 \text{ mM}$ , respectively. The steady-state kinetics for CSA formation obtained by HPLC under identical reaction conditions in D<sub>2</sub>O is overlaid on the same plot ( $\blacksquare$ ) for comparison. Here, the Michaelis–Menten parameters,  $k_{cat}$  and  $K_M$ , were determined to be  $0.65 \pm 0.05 \text{ s}^{-1}$  and  $7.0 \pm 1.3 \text{ mM}$ , respectively. Therefore, under equivalent conditions both HPLC and NMR yield nearly equivalent steady-state results. It should be noted that deuterium adversely affects both the maximal velocity of CSA formation and the apparent  $K_M$ -value obtained in steady-state assays. Michaelis–Menten parameters ( $k_{cat}$  and  $K_M$ ) obtained under identical conditions in H<sub>2</sub>O were determined to be  $1.3 \pm 0.2 \text{ s}^{-1}$  and  $2.3 \pm 0.3 \text{ mM}$ , respectively.

The efficiency at which an oxygenase enzyme incorporates one mol of O<sub>2</sub> into the product is referred to as ‘coupling’. Under steady-state conditions, the (CSA/O<sub>2</sub>)-coupling efficiency is defined as the ratio of the  $k_{cat}$  determined for CSA formation divided by the  $k_{cat}$  obtained for the rate of O<sub>2</sub>-consumption. Interestingly, D<sub>2</sub>O also has a significant impact on the (CSA/O<sub>2</sub>) coupling efficiency for CDO. The coupling efficiency of fully-modified CDO catalyzed L-Cys oxidation was previously reported as 75–80% [13]. Under identical conditions within a deuterium buffer, the observed (CSA/O<sub>2</sub>)-coupling (pD = 7.5) is significantly lower ( $41 \pm 5\%$ ). The observed  $k_{cat}$ ,  $K_M$ , and coupling efficiency all appear to be negatively influenced by substituting D<sub>2</sub>O for H<sub>2</sub>O. While beyond the scope of this study on substrate-specificity, a full report of the solvent isotope effects on CDO catalysis, oxidative coupling, and proton-inventory is described elsewhere [35].

It is also possible explanation that deuterium negatively influences the stability of the protein resulting in decreased activity. Therefore, CD spectroscopy was used to evaluate the influence of D<sub>2</sub>O on secondary structure. In these experiments, 5  $\mu$ M samples of CDO were prepared in 25 mM phosphate, 50 mM NaCl, pL 7.5, 20 °C. As illustrated in Supplemental Information, Fig. S3, the UV CD spectra [185–260 nm] of fully-modified CDO shows a maxima at 193 nm and two minima at 208 and 222 nm. Analysis of the CDO secondary structure was made by comparison to known protein standards (myoglobin, poly-L-lysine, and lysozyme) utilizing the freely available software K2D3 as described in Materials and

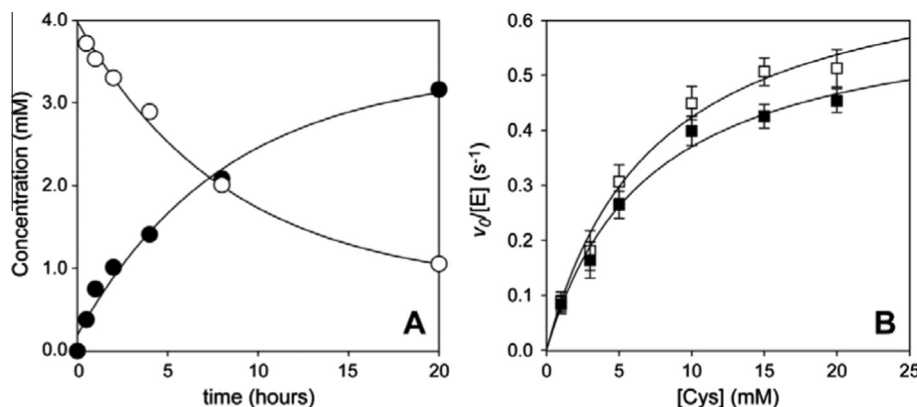


**Fig. 2.** (A) Time course of L-Cys decay and CSA formation with time. Each data set was fit to either a single exponential decay (L-Cys, white circle) or rise to maximum (CSA, black circle) using the same observed rate constant of  $k_{obs} \sim 0.12 \pm 0.03 \text{ h}^{-1}$ ; amplitude,  $4.0 \pm 0.15 \text{ mM}$  ( $\sim 84\%$  of expected). The initial velocity for CSA formation at 4.5 mM L-Cys is obtained ( $v_0/[E] = 0.27 \pm 0.07 \text{ s}^{-1}$ ) by normalizing the observed rate by the concentration of enzyme (0.5  $\mu$ M). (B) Comparative Michaelis–Menten plot for CDO catalyzed steady-state CSA formation determined by NMR ( $\square$ ) and HPLC ( $\blacksquare$ ). Assay conditions: 25 mM sodium phosphate, 50 mM NaCl, pD 7.5,  $20 \pm 2 \text{ }^\circ\text{C}$ .

methods. From this analysis, it was observed that the fraction of  $\alpha$ -helical and  $\beta$ -sheet secondary structure in buffer prepared in H<sub>2</sub>O is  $14 \pm 4\%$  and  $35 \pm 3\%$ , respectively. These values correlate well with the percent  $\alpha$ -helical (17%)  $\beta$ -sheet (34%) content determined by X-ray crystallography [10]. By comparison, no significant change is observed in the fraction of  $\alpha$ -helix (15%) or  $\beta$ -sheet (33%) observed for CDO in deuterium buffer. This result indicates that the perturbations observed in the steady-state kinetic parameters cannot be attributed to a change in the secondary structure of CDO.

While LC–MS methods for CSA detection are described in the literature, the use of tandem LC–MS/MS has not previously been demonstrated. In these experiments, both methods were utilized to verify the identity of the sulfinic acid product produced in CDO catalyzed reactions and confirm dioxygenase activity. Multiple reaction monitoring (MRM) was performed to verify CSA formation as described in Materials and methods. In these experiments, the  $[M+H]^+$  molecular ion for CSA (154  $m/z$ ) was selected for secondary fragmentation. MRM optimization was then employed to maximize transition intensity and sensitivity for each fragment allowing for quantitation of product ions. The optimized MRM method was used to verify sulfinic acid product by direct injection of enzymatic assays. These results were compared to direct injection of standards. Fig. 3 (panel A) shows the MRM spectra for a standard solution of CSA. In addition to the 154  $m/z$  parent  $[M+H]^+$  ion, two additional ions are observed at 44 and 74  $m/z$ . Fig. 3B demonstrates that direct injection (2  $\mu$ L) of the CDO catalyzed reaction with L-Cys yields and identical fragmentation pattern. The matching fragmentation pattern and relative intensities confirm the native CSA product within CDO reactions.

As final confirmation of dioxygenase activity, selected ion mode (SIM) was used to observe an appropriate shift in the observed product  $[M+H]^+$  ion upon substitution of  $^{18}\text{O}_2$  for the naturally abundant  $^{16}\text{O}_2$ . As illustrated in Fig. 3C, CDO reactions performed in the presence of  $^{18}\text{O}_2$  results in a +4  $m/z$  shift (154  $m/z$  versus 158  $m/z$ ) in the observed  $[M+H]^+$  parent ion, thus verifying the inclusion of both oxygen atoms into the L-Cys substrate as expected.

Now that all assay procedures and analytical methods have been validated for the quantitation of native substrate and product within enzyme catalyzed reactions, it is now possible to proceed to the evaluation of CDO specificity using non-native substrates.

#### Determination of steady-state CDO kinetics and coupling utilizing non-native substrates

As presented above, NMR can be used to monitor the steady-state kinetics of CDO catalyzed CSA formation with the caveat that the observed (CSA/O<sub>2</sub>)-coupling efficiency is decreased in D<sub>2</sub>O

relative to H<sub>2</sub>O. With this in mind, NMR can be used to evaluate the relative substrate specificity for CDO using a wide range of commercially available thiol-substrates. For each substrate evaluated, confirmation of dioxygenase product was independently verified by mass spectrometry using the methods described above.

#### CDO catalyzed formation of hypotaurine from 2-aminoethanethiol (cysteamine)

The NMR spectra for cysteamine and hypotaurine in D<sub>2</sub>O (pD 7.5) are shown in Supplemental Information, Fig. S4. The non-exchangeable protons on the  $\alpha$ - and  $\beta$ -carbon are observed within the spectral window (2.50–4.00 ppm). The resonances for the  $\beta$ -protons of cysteamine ( $\delta = 2.84$ , white square) and hypotaurine ( $\delta = 2.65$ , black square) are well resolved and thus can be monitored over the course of a typical reaction. Cysteamine exhibits 2 sets of resonances observed as triplets ( $t$ ) centered at 2.84 and 3.21 ppm. By comparison, the same  $\alpha/\beta$ -protons observed for hypotaurine are observed at 2.65 and 3.36 ppm. Since the  $\beta$ -protons peaks slightly overlap for substrate and product (3.21 and 3.36 ppm, respectively), the  $\alpha$ -protons were selected to monitor the progress of the CDO catalyzed reaction.

For reactions involving non-natural substrates, the concentration of CDO used in these experiments was increased to compensate for slower reaction rates. As described previously, reactions were initiated by addition of enzyme CDO (50  $\mu$ M) to a buffered D<sub>2</sub>O solution containing 90 mM cysteamine (20 °C). In these reactions, very low (*but detectable*) features associated with hypotaurine ( $\delta = 2.65$  ppm) formation could be observed in CDO reactions (Fig. S4). Steady state kinetics for CDO catalyzed hypotaurine formation was performed at varying cysteamine concentrations ranging from 25 to 100 mM. Under these conditions a linear increase in the enzyme normalized initial ( $v_0/[E]$ ) rate can be observed with increasing substrate concentration. However, even at these elevated substrate concentrations, full enzyme saturation kinetics was never observed and thus a value for  $K_M$  could not be determined for cysteamine. Regardless, from the best fit to the linear portion of the curve, the pseudo-second order rate constant (approximately  $k_{cat}/K_M$ ) was determined ( $k_{obs} \sim 0.01 \text{ M}^{-1} \text{ s}^{-1}$ ). For comparison to the product formation data, the efficiency by which CDO incorporates one mol of O<sub>2</sub> into the hypotaurine product was also determined for cysteamine reactions. Similar to product formation reactions, saturation kinetics as monitored by the Clarke-type O<sub>2</sub>-electrode is also not obtained and thus the pseudo-second order rate constant for O<sub>2</sub>-consumption was determined from the best fit to the linear portion of the curve ( $k_{obs} \sim 0.63 \text{ M}^{-1} \text{ s}^{-1}$ ). Therefore, in reactions with cysteamine, CDO exhibits >1% coupling efficiency.

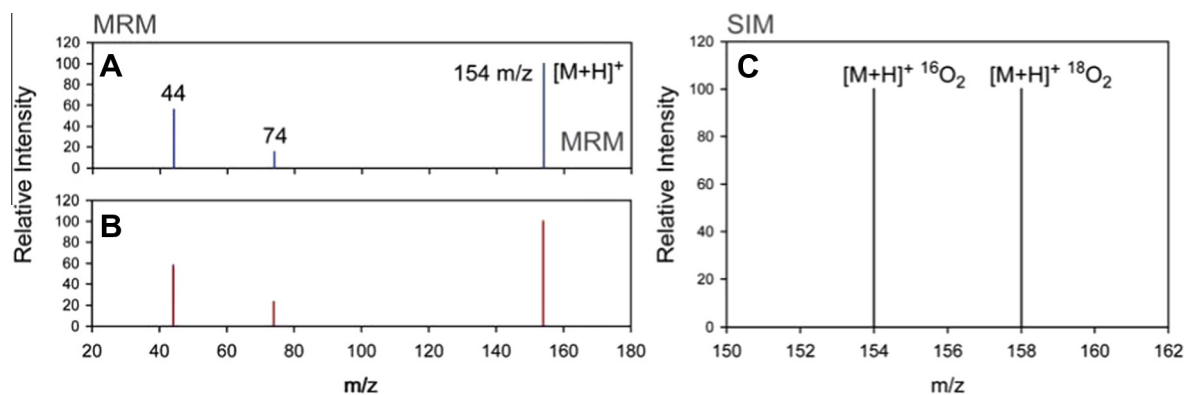


**Fig. 3.** LC–MS study on CDO's natural substrate L-cysteine using MRM (Multiple reaction monitoring) and SIM (select ion mode). (A) Blue lines represent products detected with CSA standard. (B) Red lines represent products detected with reaction sample catalyzed by CDO. (C) SIM MS illustrating the +4  $m/z$  shift in the CSA product ion peak (154–158  $m/z$ ) upon substitution of  $^{18}\text{O}_2$  for  $^{16}\text{O}_2$ . (For interpretation of the references to colour in this figure legend, the reader is referred to the web version of this article.)

Given the slow rate of catalysis and high level of oxidative uncoupling, it is not surprising that features attributed to disulfide cross-link formation can be observed in reactions with cysteamine at prolonged time-points. The chemical shifts associated with disulfide-linked cysteamine are indicated by (\*) in Fig. S4. These features are completely removed upon addition of a suitable reductant such as tris(2-carboxyethyl)phosphine hydrochloride (TCEP). Therefore, only the rate of hypotaurine formation should be considered for kinetic measurements as opposed to the decay of the cysteamine substrate.

Verification of the hypotaurine product was performed by tandem mass spectrometry (MRM) as illustrated in Fig. 4. In these experiments, the  $[M+H]^+$  molecular ion for hypotaurine (110  $m/z$ ) was selected for further fragmentation. MRM optimization was performed on a standard solution of hypotaurine and then compared to direct injections of the enzymatic reaction. In addition to the 110  $m/z$  parent  $[M+H]^+$  shown Fig. 4(panel A), the MRM spectra for a standard solution of hypotaurine exhibits three characteristic ions at 30, 45 and 65  $m/z$ . By comparison, direct injection (2  $\mu$ L) of the CDO catalyzed reaction with cysteamine yields an identical fragmentation pattern with matching intensities, thus confirming formation of the hypotaurine product within CDO reactions. Selected ion mode (SIM) was used to observe an appropriate shift in the observed product  $[M+H]^+$  ion upon substitution of  $^{18}O_2$  for the naturally abundant  $^{16}O_2$  to confirm the dioxygenase activity. As illustrated in Fig. 4B, CDO reactions performed in the presence of  $^{18}O_2$  results in a +4  $m/z$  shift (114  $m/z$  versus 110  $m/z$ ) in the observed  $[M+H]^+$  parent ion, thus verifying the inclusion of both oxygen atoms into the substrate.

#### CDO catalyzed thiol-oxidations

NMR kinetic studies with the natural L-Cys substrate and the substrate analogue cysteamine effectively illustrate the dynamic range of this analysis. While not possible in many enzymatic systems, the elevated  $K_M$  observed for CDO (6.9 mM) within  $D_2O$  allows for collection of steady-state kinetic results at substrate concentrations ranging from the NMR detection limit (0.3 mM) up to, and beyond the apparent  $K_M$  of CDO. As illustrated in Table 1, several other commercially available thiol-substrates were analyzed using the same methodology as described for L-Cys and cysteamine. In all instances, the steady-state rate of  $O_2$ -consumption and product formation was determined to determine the coupling efficiency for each substrate. When product sulfinic acid standards were not commercially available, the decrease in the substrate peak was monitored by NMR as described for Cys and cysteamine reactions. In the absence of a product standard, tandem mass

spectrometry by MRM could not be utilized for verification of product. Instead, the LC-MS (*selected ion mode*) was used to confirm appropriate parent ion mass and shift in parent ion mass (+4  $m/z$ ) in reactions where  $^{18}O_2$  was substituted for  $^{16}O_2$ . Remarkably, despite the broad range of substrates employed, all of the oxidized products generated by CDO catalyzed reactions all exhibited the appropriate +4  $m/z$  shift in  $^{18}O_2$  reactions indicating a 4 electron oxidation of the sulfur atom to produce the appropriate sulfinic acid. Other than formation of a disulfide-bond, no evidence for partial thiol-oxidation or formation of multiple products was observed.

#### Discussion

While a variety of highly sensitive methods have been described in the literature for the detection of cysteine sulfinic acid [14,36–39], NMR spectroscopy offers the most versatile means to study a variety of potential enzyme substrates under identical conditions. The high  $K_M$  value observed for CDO catalyzed reactions in  $D_2O$  (7 mM) allows for collection of data at substrate concentrations appropriate for steady-state kinetic studies. One caveat of using NMR spectroscopy is the significant decrease in the (CSA/ $O_2$ )-coupling in  $D_2O$  relative to  $H_2O$ . While beyond the scope of this manuscript, a detailed accounting of the solvent isotope effects on CDO catalysis is described elsewhere [35].

As with most oxidase and oxygenase enzymes,  $O_2$ -activation in TDO enzymes is gated by substrate-binding. Currently two theories have been proposed to explain the substrate-gated  $O_2$  regulation exhibited by non-heme mononuclear iron enzymes; (1) thermodynamic gating of the  $Fe^{II}/Fe^{III}$  redox couple and (2) Fe-site conformational changes which facilitate direct  $O_2$ -coordination [40–42]. Taking the structure of the substrate-bound active site into consideration (Fig. 1), the data provided in Table 1 suggest that simultaneous coordination of both the substrate-thiol and amine groups are necessary for gating  $O_2$ -binding and subsequent substrate oxidation. For example, 1-mercaptopropane (1MP) and 3-mercaptopropionic acid (3MP) lack an amino group and thus neither  $O_2$ -consumption or sulfinic acid product formation is observed upon addition to aerobic solutions of CDO. The fact that CDO is unable to oxidize 3MP, suggests that CDO may also have a means by which to discriminate between O- and N-atom Fe-coordination. While 2-(dimethylamino)ethanethiol (DME) has an available amino functional group, the increased steric bulk and altered pKa of the alkylated amine relative to the primary Cys-amine clearly inhibits direct Fe-coordination. While the activity was too low for accurate kinetic measurements, LC-MS clearly identifies a sulfinic

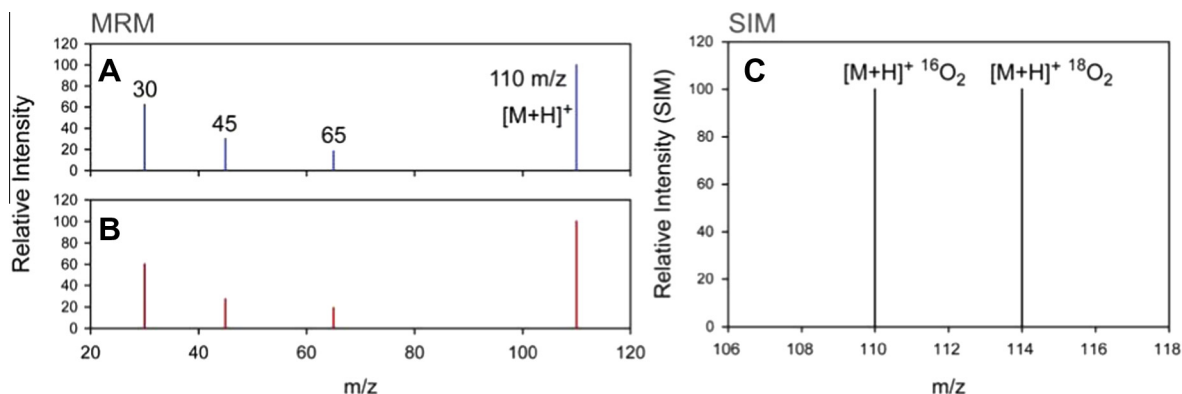


**Fig. 4.** LC-MS study on CDO's non-natural substrate cysteamine using MRM (Multiple reaction monitoring) and SIM (select ion mode). (A) Blue lines represent products detected with hypotaurine standard. (B) Red lines represent products detected with reaction sample catalyzed by CDO. (C) SIM MS illustrating the +4  $m/z$  shift in the hypotaurine product ion peak (110–114  $m/z$ ) upon substitution of  $^{18}O_2$  for  $^{16}O_2$ . (For interpretation of the references to colour in this figure legend, the reader is referred to the web version of this article.)

**Table 1**  
Steady-state kinetic parameters determined by NMR and O<sub>2</sub>-electrode for selected CDO substrates.

Substrate	Oxygen consumption			Product formation			
	$k_{cat}$ (s <sup>-1</sup> )	$K_M$ (mM)	$V/K$ (M <sup>-1</sup> s <sup>-1</sup> )	$k_{cat}$ (s <sup>-1</sup> )	$K_M$ (mM)	$V/K$ (M <sup>-1</sup> s <sup>-1</sup> )	Coupling (%)
L-Cys	1.8 ± 0.02	0.70 ± 0.2	2570	0.74 ± 0.06	7.0 ± 1.3	106 ± 21	41%
D-Cys	2.4 ± 0.04	3.1 ± 0.2	770	0.08 ± 0.02	6.8 ± 3.2	9 ± 5	3.3%
L-PA	1.0 ± 0.27	34.6 ± 8.0	30	0.07 ± 0.03	6.2 ± 2.1	10 ± 5	4.8%
L-Hcy	0.2 ± 0.01	13.4 ± 1.8	119	N/A	N/A	0.3 ± 0.1	5.6%
CA	N/A	N/A	0.63	N/A	N/A	<0.01	0.9%
MS	–	N/A	N/A	–	N/A	N/A	N/A
CME	+	N/A	N/A	+	N/A	N/A	N/A
SC	–	N/A	N/A	–	N/A	N/A	N/A
DME	–	N/A	N/A	–	N/A	N/A	N/A
3MP	–	N/A	N/A	–	N/A	N/A	N/A
1MP	–	N/A	N/A	–	N/A	N/A	N/A

In these experiments,  $k_{cat}$  is defined as  $v_0/[E]$ . Substrate abbreviations: Cys, Cysteine; Hcy, homocysteine; CA, 2-aminoethanethiol (*cysteamine*); MS, mercaptosuccinate; PA, L-penicillamine, CME, L-cysteine methyl ester; DME, 2-(dimethylamino)ethanethiol. SC, S-methyl-L-cysteine; 3MP, 3-mecaptopropionate, 1MP; 1-mecaptopropane.

acid product in reactions with L-cysteine methyl ester (CME). By contrast, the methylated thiol group of S-methyl-L-cysteine (SC) prevents S-atom coordination to the Fe-site; thus catalysis is not possible. As most of these substrates are isosteric with L-Cys, it is expected that they would induce a similar conformational changes upon docking within the active site. Therefore, at least qualitatively, the results presented here support the hypothesis that simultaneous (S/N)-bidentate coordination of the CDO substrates thermodynamically regulate O<sub>2</sub>-binding by altering the Fe<sup>III/II</sup> redox couple.

One feature that is becoming increasingly apparent is the role of the C93-Y157 pair in providing appropriate substrate orientation and stereoselectivity. The (S/N)-bidentate substrate coordination provides two points of simultaneous interaction. A third point of interaction is produced by hydrogen bonding between the Cys-carboxylate group and the C93-Y157 pair (2.94 Å). This third interaction is also stabilized electrostatically by interaction with R60 (separated by 2.91–3.16 Å). Collectively, these interactions satisfy the “three point interaction rule” for chiral selection [43]. Assuming bidentate coordination of the substrate is the only requirement for gating reactivity with O<sub>2</sub>, then addition of either D- or L-isomers should trigger consumption of O<sub>2</sub>, which is indeed what is observed experimentally. Despite this, as shown in Fig. 5A, the ratio of O<sub>2</sub>-consumed per CSA generated is vastly attenuated (< 3%) in reactions involving D-Cys as compared to the physiologically relevant L-Cys substrate (~40%). Similar uncoupling effects have also been reported in the absence of D<sub>2</sub>O (81% and 4% respectively). Indeed, nearly a 10-fold increase is observed in specificity ( $V/K$ ) of CDO for L-Cys as compared to D-Cys [13]. This suggests that, in addition to the chiral selection provided by three simultaneous points of interaction, outer-sphere interactions with C93-Y157/R60 residues may influence the geometry of the (O<sub>2</sub>/Substrate)-bound ternary enzyme complex to minimize escape of partially reduced reactive

oxygen species. This hypothesis is supported by previous EPR studies using cyanide as a spectroscopic probe for substrate-interactions within the catalytically inert Fe<sup>III</sup>-CDO. In these experiments, both D- and L-Cys were capable of binding the active site to facilitate cyanide binding, however samples prepared from D-Cys exhibited significantly greater *g*-strain suggesting greater conformational heterogeneity [13]. Reactions with cysteamine further support this model in that both O<sub>2</sub>-consumption and hypotaurine formation are significantly decreased. Moreover, as illustrated in Fig. 5B, under identical conditions, the specificity ( $V/K$ ) of CDO for cysteamine is four orders of magnitude less than that observed for L-Cys (<0.01 M<sup>-1</sup> s<sup>-1</sup>). Thus in the absence of a third point of interaction within the CDO active site pocket, substrate binding appears to be weak resulting in attenuated O<sub>2</sub>-consumption rates, enzymatic specificities, and coupling efficiencies.

CDO reactions with homocysteine and L-penicillamine (PA) appear to also support this model in that both substrates have the capacity to coordinate via bidentate (S/N)-ligation as well as satisfy the ‘three point interaction’ with CDO. Therefore it is not surprising that the rate of O<sub>2</sub>-consumption observed for PA (1.0 s<sup>-1</sup>) is quite similar to both L/D-Cys. Moreover, the specificity of CDO for these substrates is an order of magnitude greater than cysteamine. Unlike PA, homocysteine exhibits low O<sub>2</sub>-consumption rate (0.2 s<sup>-1</sup>). Presumably, the increased steric bulk of these substrates distort the geometry of the ternary complex resulting in decreased productive catalysis (8% and 15% relative to L-Cys). Within experimental error, CDO specificity for D-Cys and PA is essentially equivalent (9 <  $V/K$  < 10 M<sup>-1</sup> s<sup>-1</sup>). This value is an order of magnitude lower than observed for the native L-Cys substrate. By contrast, CDO specificity for homocysteine (0.3 M<sup>-1</sup> s<sup>-1</sup>) is vastly lower than observed for L-Cys. In principle, the additional (CH<sub>2</sub>)-group within the homocysteine side chain significantly increased the steric bulk within the active site pocket thus distorting substrate-enzyme

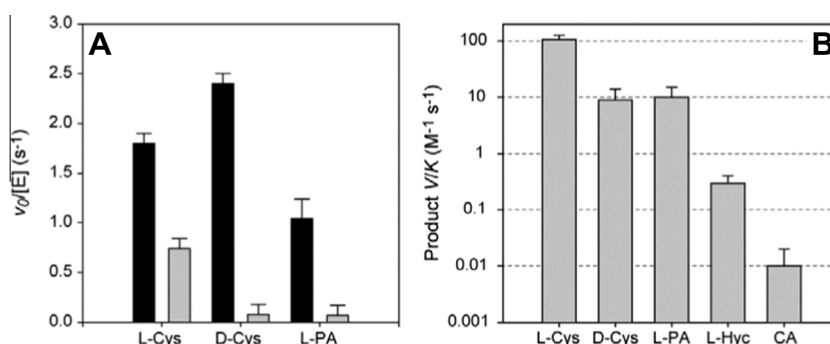


**Fig. 5.** Values determined for CDO  $k_{cat}$  ( $v_0/[E]$ ) and specificity ( $V/K$ ) for selected substrates. (A) The maximum rate of O<sub>2</sub>-consumption (black bars) and product formation (gray bars) reflect the impact of substrate on enzymatic coupling. Enzyme specificity ( $V/K$ ) for each substrate is indicated by the gray bars in panel B.

interactions. Interestingly, the oxidative coupling observed for homocysteine is quite similar to that observed for D-Cys and PA.

Given the absence of a carboxylate group on cysteamine, it seems unlikely that ADO would require a Cys-Tyr cross-link to orientate substrate binding. Indeed, sequence comparison of mammalian ADO and CDO enzymes suggest the absence of a Cys-Tyr pair at an equivalent position in the CDO sequence. Nevertheless, it has been reported that SDS PAGE of ADO isolated from specific mouse tissue extracts exhibited a doublet (or triplet) protein band similar to what is observed for mammalian CDO [44]. This feature is absent in homogeneously purified recombinant SUMO- or Flag-tagged ADO and thus this may simply be the result of post-translational ubiquitination as suggested by the authors.

In the absence of any structural information for thiol dioxygenase enzymes other than CDO, it is difficult to fully consider the relevance of outer-sphere interactions relevant to thiol dioxygenase substrate specificity. As a first approximation, the structural threading model for the *M. musculus* ADO shown in **Supplemental Information (Fig. S5)** was generated using the substrate-bound *Rattus norvegicus* CDO crystal structure (pdb code 3ELN) as a template [45,46]. While homology models should be considered with appropriate skepticism, they do provide a reasonable framework for the discussion of conserved residues within the enzyme active site and potential substrate interactions. Within the ADO homology model, H155 and Y157 are replaced by D192 and L194 as indicated by sequence alignment. The increased hydrophobicity of the ADO active site pocket likely facilitates cysteamine binding to the Fe-site as no other competing hydrogen-bonding interactions are present. The only Cys and Tyr residues in close enough proximity to produce a covalent cross-link are Y162 and C169 but these do not overlap with the C93-Y157 pair of CDO (3ELN). Furthermore, these residues appear quite distant from the predicted 3-His active site (H100, H102, and H179) (~10 Å). Thus, if C162 and Y169 do indeed form a covalent cross-link analogous to CDO, it is difficult to see how they would be catalytically relevant on the basis of this model.

The work presented here provides a much needed evaluation of the minimum substrate requirements necessary for CDO catalyzed O<sub>2</sub>-activation, sulfinic acid formation, and coupling efficiency. Substrates were selected to evaluate cross-reactivity with other thiol-dioxygenase enzyme substrates as well as provide insight into potential substrate-active site interactions for CDO.

## Acknowledgments

This work was supported by NSF (CHE) 1213655 to B.S.P. We would also like to acknowledge NSF financial support (CRIF:MU CHE-0840509) for the purchase of the JEOL ECA500 500 MHz FT-NMR spectrometers and the UTA Shimadzu Center for Advanced Analytical Chemistry for the use of HPLC and LC-MS/MS instrumentation.

## Appendix A. Supplementary data

Supplementary data associated with this article can be found, in the online version, at <http://dx.doi.org/10.1016/j.abb.2014.11.004>.

## References

- [1] K.G. Reddie, K.S. Carroll, *Curr. Opin. Chem. Biol.* 12 (2008) 746–754.
- [2] P.G. Winyard, C.J. Moody, C. Jacob, *Trends Biochem. Sci.* 30 (2005) 453–461.
- [3] D. Trachootham, J. Alexandre, P. Huang, *Nat. Rev. Drug Discov.* 8 (2009) 579–591.
- [4] D.P. Behave, W.B. Muse, K.S. Carroll, *Infect. Disord. Drug Targets* 7 (2007) 140–158.
- [5] C. Gordon, H. Bradley, R.H. Waring, P. Emery, *Lancet* 339 (1992) 25–26.
- [6] C.R. Simmons, L.L. Hirschberger, M.S. Machi, M.H. Stipanuk, *Protein Expr. Purif.* 47 (2006) 74–81.
- [7] M.T. Heafield, S. Fearn, G.B. Steventon, R.H. Waring, A.C. Williams, S.G. Sturman, *Neurosci. Lett.* 110 (1990) 216–220.
- [8] S.C. Chai, A.A. Jerkins, J.J. Banik, I. Shalev, J.L. Pinkham, P.C. Uden, M.J. Maroney, *J. Biol. Chem.* 280 (2005) 9865–9869.
- [9] P.J. Bagley, L.L. Hirschberger, M.H. Stipanuk, *Anal. Biochem.* 227 (1995) 40–48.
- [10] C.M. Driggers, R.B. Cooley, B. Sankaran, L.L. Hirschberger, M.H. Stipanuk, P.A. Karplus, *J. Mol. Biol.* 425 (2013) 3121–3136.
- [11] E. Siakkou, M.T. Rutledge, S.M. Wilbanks, G.N.L. Jameson, *Biochim. Biophys. Acta* 1814 (2011) 2003–2009.
- [12] J.E. Dominy Jr., J. Hwang, S. Guo, L.L. Hirschberger, S. Zhang, M.H. Stipanuk, *J. Biol. Chem.* 283 (2008) 12188–12201.
- [13] W. Li, E.J. Blaesi, M.D. Pecore, J.K. Crowell, B.S. Pierce, *Biochemistry* 52 (2013) 9104–9119.
- [14] J.A. Crawford, W. Li, B.S. Pierce, *Biochemistry* 50 (2011) 10241–10253.
- [15] B.S. Pierce, J.D. Gardner, L.J. Bailey, T.C. Brunold, B.G. Fox, *Biochemistry* 46 (2007) 8569–8578.
- [16] J.E. Dominy Jr., C.R. Simmons, P.A. Karplus, A.M. Gehring, M.H. Stipanuk, *J. Bacteriol.* 188 (2006) 5561–5569.
- [17] M. Stipanuk, C. Simmons, P. Andrew Karplus, J. Dominy, *Amino Acids* (2010) 1–12.
- [18] N. Bruland, J.H. Wubbeler, A. Steinbuechel, *J. Biol. Chem.* 284 (2009) 660–672.
- [19] U. Brandt, C. Waletzko, B. Voigt, M. Hecker, A. Steinbuechel, *Appl. Microbiol. Biotechnol.* 98 (2014) 6039–6050.
- [20] S. Ye, X. Wu, L. Wei, D. Tang, P. Sun, M. Bartlam, Z. Rao, *J. Biol. Chem.* 282 (2007) 3391–3402.
- [21] C.W. Njeri, H.R. Ellis, *Arch. Biochem. Biophys.* 558 (2014) 61–69.
- [22] C.R. Simmons, Q. Liu, Q. Huang, Q. Hao, T.P. Begley, P.A. Karplus, M.H. Stipanuk, *J. Biol. Chem.* 281 (2006) 18723–18733.
- [23] M.H. Stipanuk, *Annu. Rev. Nutr.* 24 (2004) 539–577.
- [24] L. Ewertz, B. Sorbo, *Biochim. Biophys. Acta* 128 (1966) 296–305.
- [25] B. Soerbo, L. Ewertz, *Biochem. Biophys. Res. Commun.* 18 (1965) 359–363.
- [26] J.B. Lombardini, T.P. Singer, P.D. Boyer, *J. Biol. Chem.* 244 (1969) 1172–1175.
- [27] C.H. Misra, *Neurochem. Res.* 8 (1983) 1497–1508.
- [28] J.D. Gardner, B.S. Pierce, B.G. Fox, T.C. Brunold, *Biochemistry* 49 (2010) 6033–6041.
- [29] P.K. Glasoe, F.A. Long, *J. Phys. Chem.* 64 (1960) 188–190.
- [30] N.J. Greenfield, *Nat. Protoc.* 1 (2007) 2876–2890.
- [31] J.A. Dean (Ed.), *Lange's Handbook of Chemistry*, 14 ed., McGraw-Hill Inc, New York, 1992.
- [32] R.A. Yost, D.D. Fetterolf, *Mass Spectrom. Rev.* 2 (1983) 1–45.
- [33] A.L. Corder, B.P. Subedi, S. Zhang, A.M. Dark, F.W. Foss, B.S. Pierce, *Biochemistry* 52 (2013) 6182–6196.
- [34] A. Kasperova, J. Kunert, M. Horynova, E. Weigl, M. Sebela, R. Lenobel, M. Raska, *Mycoses* 54 (2011) e456–462.
- [35] J.K. Crowell, W. Li, B.S. Pierce, *Biochemistry* (2014), <http://dx.doi.org/10.1021/bi501241d> (in press).
- [36] E. Siakkou, S.M. Wilbanks, G.N. Jameson, *Anal. Biochem.* 405 (2010) 127–131.
- [37] S. Heron, M.G. Maloumbi, M. Dreux, E. Verette, A. Tchaplaj, *J. Chromatogr. A* 1161 (2007) 152–156.
- [38] T. Bantan-Polak, M. Kassai, K.B. Grant, *Anal. Biochem.* 297 (2001) 128–136.
- [39] P.J. Hillas, P.F. Fitzpatrick, *Biochemistry* 35 (1996) 6969–6975.
- [40] E.I. Solomon, T.C. Brunold, M.I. Davis, J.N. Kemsley, S.-K. Lee, N. Lehnert, F. Neese, A.J. Skulan, Y.-S. Yang, J. Zhou, *Chem. Rev.* 100 (2000) 235–349.
- [41] E.I. Solomon, A. Decker, N. Lehnert, *Proc. Natl. Acad. Sci. U.S.A.* 100 (2003) 3589–3594.
- [42] M. Costas, M.P. Mehn, M.P. Jensen, L.J. Que, *Chem. Rev.* 104 (2004) 939–986.
- [43] L.H. Easson, E. Stedman, *Biochem. J.* 27 (1933) 1257–1266.
- [44] J.E. Dominy Jr., C.R. Simmons, L.L. Hirschberger, J. Hwang, R.M. Coloso, M.H. Stipanuk, *J. Biol. Chem.* 282 (2007) 25189–25198.
- [45] L.A. Kelley, M.J. Sternberg, *Nat. Protoc.* 4 (2009) 363–371.
- [46] C.R. Simmons, K. Krishnamoorthy, S.L. Granett, D.J. Schuller, J.E. Dominy, T.P. Begley, M.H. Stipanuk, P.A. Karplus, *Biochemistry* 47 (2008) 11390–11392.